A Profile of the Residues in the First Intracellular Loop Critical for Gs-Mediated Signaling of Human Prostacyclin Receptor Characterized by an Integrative Approach of NMR-Experiment and Mutagenesis†

Lihai Zhang, Gangxiong Huang, Jiaxin Wu, and Ke-He Ruan*

Vascular Biology Research Center and Division of Hematology, Department of Internal Medicine, The University of Texas Health Science Center, Houston, Texas 77030

Received March 15, 2005; Revised Manuscript Received July 1, 2005

ABSTRACT: The first intracellular loop (iLP1, residues 39−51) of human prostacyclin receptor (IP) was proposed to be involved in signaling via its interaction with the Gαs protein. First, evidence of the IP iLP1 interaction with the C-terminus of the Gαs protein was observed by the fluorescence and NMR spectroscopy using the synthetic peptide (Gαs-Ct) mimicking the C-terminal 11 residues of the Gαs protein in the presence of a constrained synthetic peptide mimicking the IP iLP1. Then, the residues (Arg42, Ala44, and Arg45) in the IP iLP1 peptide possibly involved in contacting the Gαs-Ct peptide were initially assigned by observation of the significant proton resonance shifts of the side chains of the constrained IP iLP1 peptide using 2D ^{1}H NMR spectroscopy. The results of the NMR studies were used as a guide for further identification of the residues in the IP important to the receptor signaling using a recombinant protein approach. A profile of the residues in the IP iLP1, including the residues observed from the NMR studies involved in the Gαs mediated signaling, was mapped out by mutagenesis. According to our results, it can be predicted that the seven residues (Arg42−Ala48) with the conserved Arg45 at the center will form an epitope with a specific conformation involved in the Gαs mediated signaling. The conservation of the basic residues (Arg45 in the IP) in all of the prostanoid receptors suggests that the iLP1 regions of the other prostanoid receptors may also contain the epitopes important to their signaling.

Prostacyclin (prostaglandin I_2 (PGI_2[1])) is one of the prostanoids that include thromboxane A_2 (TXA_2), prostaglandins D_2 (PGD_2), E_2 (PGE_2), and F_2 (PGF_2) that are synthesized by vascular smooth muscle, endothelium, and other tissues. TXA_2 is a potent stimulator of platelet aggregation and a smooth muscle constrictor. PGI_2 actions are functionally antagonistic to those of TXA_2. Functions of the prostanoids are mediated by their specific receptors that belong to the G protein-coupled receptor (GPCR) family, with seven transmembrane (TM) domains coupled to different G proteins. The human PGI_2 receptor (IP) gene was first cloned in 1994 (*1*). The IP receptor mainly coupled to the heterotrimeric Gs protein with an increase of the intracellular cAMP level has been identified (*2*).

Biochemical and molecular approaches have defined several features of the interaction between the IP receptor and the G protein: (1) The IP receptor mainly interacts with the α subunit of heterotrimeric Gs protein (Gαs), and probably interacts with α subunit of heterotrimeric Gq protein (Gαq) as well (*3*). (2) The C-terminal region of Gαs (at least the last 11 residues) could interact directly with the many GPCRs (*4*−*13*). (3) G protein coupling is thought to be mediated by an interaction of several intracellular domains of a GPCR, including the intracellular loops and/or carboxyl-terminus. However, little information is available for the defined specific residues involved in G protein coupling in the IP receptor. For example, Hayes et al. found that the end of the C-terminal tail of the IP receptor may be important for the heterotrimeric Gs protein coupling (*14*), but evidence from a separate group (*15*) showed that this region may not be so essential. It is clear that the characterization of the heterotrimeric Gs protein coupling site in the intracellular domains of the IP receptor is important for the resolution of this controversy.

A natural mutation of the human TP receptor with Arg60 to Leu impaired the receptor function and caused a bleeding disorder (*16*). Very recently, the Arg60 located in the first intracellular loop (iLP1) was confirmed by our NMR spectroscopic studies using a constrained synthetic peptide mimicking the iLP1 segment. The Arg60 residue involved in Gαq coupling, which mediates increasing intracellular calcium levels, has also been identified using the recombinant TP receptors with the mutants of Arg60Leu and Arg60Lys (*17*). Interesting observations, such as the replacement of

†This work was supported in part by HL56712 and HL079389.

* To whom correspondence should be addressed. Division of Hematology, Department of Internal Medicine, University of Texas Health Science Center at Houston, 6431 Fannin St., Houston, TX 77030. Tel.: 713-500-6769. Fax: 713-500-6810. E-mail: kruan@uth.tmc.edu.

[1] Abbreviations: EP, prostaglandin E_2 receptor; DP, prostaglandin D_2 receptor; FP, prostaglandin F_2 receptor; IP, prostacyclin (prostaglandin I_2) receptor; TP, thromboxane A_2 receptor; IP iLP1, the first intracellular loop of prostacyclin receptor; IP-wt, wild-type IP receptor; G protein, guanine nucleotide binding protein; Gt, transducin; EIA, enzyme immunoassay; NMR, nuclear magnetic resonance; DQF−COSY, double-quantum filtered correlation spectroscopy; TOCSY, total correlation spectroscopy; NOESY, nuclear Overhauser effect spectroscopy; PGI_2, prostaglandin I_2; HPLC, high-performance liquid chromatography; hCys or hC, homocysteine.

10.1021/bi050483p CCC: $30.25
Published on Web 08/05/2005

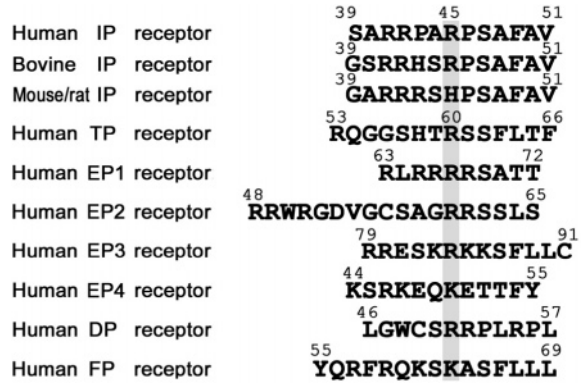

FIGURE 1: Sequence alignment of the iLP1s of the prostanoid receptors. The conserved basic residues were highlighted. The alignment was performed by Insight II program on SGI workstation.

the Arg60 with Lys could not completely restore the Gαq coupling activity of the TP receptor, have led to the conclusion that other chemical properties of the Arg side chains and its local conformation are also involved for the heterotrimeric Gs coupling beside the charge contact (*17*). This basic residue is conserved in all of the prostanoid receptors with an identical Arg residue or a similar basic residue of Lys (Figure 1). This led us to hypothesize that the basic residue and the iLP1s of other prostanoid receptors may also be involved in their specific G protein coupling. A scenario such as whether the IP receptor coupled differently to the Gs when compared to the TP receptor coupled to the Gq is a suitable test for the hypothesis. In this paper, an approach integrating NMR peptide experiments and the receptor protein mutagenesis was used to characterize the structure/function relationship of the residues important to the heterotrimeric Gs-mediated signaling while focusing on the IP iLP1 region. The interaction of the synthetic constrained peptide mimicking the IP iLP1 with the C-terminal domain of Gαs protein was determined by fluorescence and 2D NMR spectroscopic studies, and the possible residues in the IP iLP region important to the receptor signaling through Gαs coupling were predicted by NMR assignment. Mapping of the residues important to the receptor signaling in the iLP1 region in the IP protein was performed. The complete profile of the residues in the IP iLP involved in signaling through Gs coupling was identified.

EXPERIMENTAL PROCEDURES

Materials. [^{3}H] iloprost (16 Ci/mmol), unlabeled (cold) iloprost, and the cAMP Biotrak Enzyme immunoassay (EIA) kit were purchased from Amersham Biosciences (Piscataway, NJ). The QIAprep spin miniprep kit was from Qiagen (Valencia, CA). COS-7 cell was purchased from ATCC (Manassas, VA). Medium for culturing COS-7 cells was from Invitrogen (Carlsbad, CA). Ethanol-d_6 and D_2O were purchased from Cambridge Isotope Laboratories, Inc. (Andover, MA).

Peptide Synthesis. A constrained loop peptide mimicking the sequence of the putative IP iLP1 (residues 39−51) with homocysteine (hCys) residues added at both ends (Figure 2) was synthesized by fluorenylmethoxycarbonyl-polyamide solid phase method and constrained by the formation of disulfide bound as described previously (*18*). Briefly, the peptide was purified to homogeneity by HPLC after the

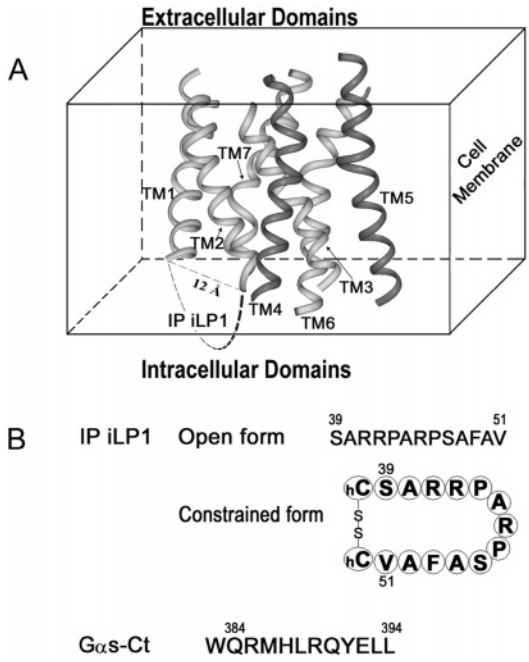

FIGURE 2: Sequences of synthetic peptides mimicked human IP iLP1 and the segments of Gαs. (A) TM domain model of human IP receptor (*27*). (B) Amino acid sequence of the constrained IP iLP1 with a disulfide bond connection through the added hCys residues at the C- and N-termini, and amino acid sequence of Gαs-Ct peptide.

synthesis. For the cyclization, the purified peptide was dissolved in 1 mL of dimethyl sulfoxide and added to H_2O at a final concentration of 0.02 mg/mL with pH 8.5 adjusted by addition of triethylamine. The peptide solution was stirred overnight at room temperature. The cyclic peptide was then lyophilized and purified by HPLC on the C4 column. A constrained loop peptide mimicking the TP iLP1 was also synthesized as a control (*17*). In addition, a Gαs-Ct peptide, mimicking the sequence of the C-terminal region (residues 384−394) of the α subunit of the heterotrimeric Gαs protein, with a Trp residue added at N-terminus (Figure 2B), was also synthesized and purified by HPLC.

Fluorescence Spectroscopic Studies for the Interaction of the Synthetic IP iLP1 Peptide and the Gαs-Ct Peptide. The interaction between the Gαs-Ct peptide and the synthetic constrained IP iLP1 peptide was monitored by fluorescence spectroscopic studies as described (*19*). The Gαs-Ct peptide was dissolved in 600 μL of sodium phosphate buffer (0.01 M, pH 7.2) containing 0.1 M NaCl, with a final concentration of 5 μM. The fluorescence intensity of the Tyr residue in the Gαs-Ct peptide was monitored fluorometrically at 279.6 nm for excitation and 303 nm for emission, in the absence or presence of the increasing concentration of the synthetic IP iLP1 or TP iLP1 peptide using a spectrofluorophotometer (Shimadzu, RF-5301PC) at room temperature in a 1.0-cm-path-length cell. Single-site binding of the IP iLP1 or TP iLP1 peptide to the Gαs-Ct peptide was fitted to the following equation (*20*):

$$F_{obs} - F_o = (F_f - F_0)\{R_t + G_t + K_d - [(R_t + G_t + K_d)^2 - 4R_tG_t]^{1/2}\}/(2G_t) \quad (1)$$

in which F_{obs} is the observed fluorescence intensities; the F_0 and F_f are the initial and final fluorescence intensities,

respectively; G_t is the total concentration of the Gαs-Ct peptide; and R_t is the total concentration of the IP iLP1 or TP iLP1 peptide. The normalized fluorescence (NF) can be calculated from

$$\mathrm{NF} = F_{obs}/F_0 = 1 + (F_f/F_0 - 1)\{R_t + G_t + K_d - [(R_t + G_t + K_d)^2 - 4R_tG_t]^{1/2}\}/(2G_t) \quad (2)$$

The titration data, normalized fluorescence (NF), and R_t were fitted by adjusting K_d and F_f using the Origin 6.1 program (OriginLab, Inc., Northampton, MA).

NMR Sample Preparation. For 2D NMR spectroscopic studies, the peptide sample of the HPLC-purified, constrained IP iLP1 peptide or Gαs-Ct peptide was dissolved in 0.5 mL sodium phosphate buffer (20 mM, pH 6.0), containing 10% D_2O and 5% ethanol-d_6, with a final concentration of 5.4 mM or 8.4 mM, respectively (*14*). The concentration for the mixture of the IP iLP1 and Gαs-Ct peptides was the same as above. For the 1D ^{1}H NMR titration experiments, different amounts (50 ∼ 3000 μM) of the IP iLP1 peptide were added to the fixed amount (100 μM) of Gαs-Ct peptide under the same conditions as the 2D NMR experiments.

NMR Experiments. Proton NMR experiments were carried out on a Bruker AMX-600 spectrometer. 2D ^{1}H NMR experiments including DQF−COSY, TOCSY, and NOESY were performed for the IP iLP1, Gαs-Ct, or their mixture at 298 K. The WATERGATE method was used to suppress the signal of water. NOESY spectra were recorded with a mixing time of 200 ms. TOCSY spectra were carried out with decoupling in the presence of scalar interactions spin-lock sequence with a total mixing time of 50 ms. A total of 512 t1 increments were used in F1 with 32 scans per t1 increment and composed of 2048 complex points in F2 in all experiments. Quadrature detection was achieved in F1 by the states-time proportional phase increment 150 zero-filled to 2048 × 2048 before Fourier transformation, and 0° (for DQF−COSY) or 90° (for TOCSY and NOESY) shifted sinbell2 window function was used in both dimensions. Ethanol-d_6 Peak was used as the reference for chemical shifts. The chemical shift and sequence-specific assignments were obtained using standard methods (*21*), auto-assignment software (*17*), and a Peakfit v4.2 program (Seasolve software, Inc., Framingham, MA).

Proton 1D NMR Titration Analysis in Fast Exchange. One-to-one binding of the IP ILP1 peptide [R], and the Gαs-Ct peptide [G], to form a peptide−peptide complex, RG, can be expressed as (*22*)

$$\text{IP ILP1} + \text{Gαs-Ct} \underset{K_{off}}{\overset{K_{on}}{\rightleftharpoons}} \text{RG} \quad (3)$$

The equilibrium dissociation constant, K_d, for this reaction is

$$K_d = k_{off}/k_{on} = ([R][G])/[RG] \quad (4)$$

Where [R] is the concentration of the IP iLP1 peptide, [G] is the concentration of the Gαs-Ct peptide, and [RG] is the concentration of the peptide−peptide complex; $R_t = [R] + [RG]$ and $G_t = [G] + [RG]$, K_d and [RG] can be calculated from

$$K_d = (R_t - [RG])\,(G_t - [RG])/[RG] \quad (5)$$

$$[RG] = (1/2)\{R_t + G_t + K_d - [(R_t + G_t + K_d)^2 - 4R_tG_t]^{1/2}\} \quad (6)$$

If $1/\tau$, the rate of the equilibration defined by eq 3, is faster than the difference in chemical shifts between free and bound ($\delta_b - \delta_f$) statuses of Gαs-Ct peptide, then the fast exchange condition exists and $\delta_{obs} = \delta_f f_f + \delta_b f_b$, where δ_f is the chemical shift of the unbound species, δ_b is that of the bound species, and f_f and f_b are the fractions unbound and bound, respectively (*22*); $f_f + f_b = 1$. The observed chemical shift during the titration of the free Gαs-Ct peptide with IP iLP1 peptide is given by

$$\delta_{obs} = \delta_f f_f + \delta_b f_b = \delta_f(1 - f_b) + \delta_b f_b = \delta_f + (\delta_b - \delta_f) f_b = \delta_f + (\delta_b - \delta_f)[RG]/G_t \quad (7)$$

After substitution of eq 7 into eq 6, the proton chemical shift perturbation ($\Delta\delta_{obs}$) is given by

$$\Delta\delta_{obs} = (\delta_{obs} - \delta_f) = (\delta_b - \delta_f)\{R_t + G_t + K_d - [(R_t + G_t + K_d)^2 - 4R_tG_t]^{1/2}\}/(2G_t) \quad (8)$$

Therefore the percentage of the proton chemical shift perturbation (F) is given by

$$F = 100\Delta\delta_{obs}/(\delta_b - \delta_f) = 100\{R_t + G_t + K_d - [(R_t + G_t + K_d)^2 - 4R_tG_t]^{1/2}\}/(2G_t) \quad (9)$$

The titration data, F and R_t, were fitted by adjusting K_d using the Origin 6.1 program (OriginLab, Inc., Northampton, MA).

PCR Cloning of the IP Receptor. PCR cloning was used to isolate the full-length cDNA of the IP receptor from human lung cDNA library obtained from Invitrogen (Carlsbad, CA). The PCR primers were designed based on human IP cDNA with modifications. The primer sequences used were 5′-ATTCTCGAGATGGCGGATTCGTGCAGGAAC-3′ (forward) and 5′-AAGAATTCACAGGGTCAGCTTGAAATGTCAG-3′ (reverse), with *Xho*I and *Eco*RI sites on the ends. The full-length cDNA of the IP receptor was obtained from standard PCR amplification that was performed in 50 μL of reaction mixture containing 1 unit of polymerase (New England Biolabs, Beverly, MA), 0.4 μM of each primer, and 2 μL of human lung cDNA for 30 cycles of 98 °C for 1 min, 60 °C for 1 min, and 72 °C for 1 min. The amplified products were isolated from agarose gel and subcloned into the *Xho*I/*Eco*RI sites of pAcSG His NT-A transfer vector (Pharmingen, San Diego, CA). Correct cDNA sequence of the receptor was confirmed by restriction enzyme digestions and DNA sequencing analysis using the Sanger dideoxy chain termination method (*23*).

Site-Directed Mutagenesis. A pAcSG-IP wild-type cDNA cloned by our laboratory was first subcloned into *Eco*RI/*Xho*I sites of pcDNA3.1(−) expression vector to generate the plasmid of pcDNA:hIP. The IP receptor mutations were then constructed by standard PCR using pcDNA3.1(−) vector with wild-type IP receptor as a template and two synthetic oligonucleotide primers containing the desired point mutation. The primers, which were complementary to opposite strands of the template, extended during the temperature cycling (95 °C for 30 s, 53 °C for 1 min 30 s, and 68 °C for 13 min) for a total of 25 cycles with an

additional extension cycle of 68 °C for 10 min using *Pfu* DNA polymerase from Stratagene (La Jolla, CA). The mutation products were treated with *Dpn*I endonuclease (Stratagene) to digest the parental DNA template and confirmed by DNA sequencing. The plasmids were then prepared using Midiprep kit (Qiagen) for the transfection into COS-7 cells.

Expression of the Recombinant IP Receptor in COS-7 Cells. COS-7 cells, placed on 100-mm dishes at a density of 2.0×10^6, were cultured overnight, at 37 °C in a humidified 5% CO_2 atmosphere in high-glucose Dulbecco's modified Eagle's medium containing 10% fetal bovine serum, antibiotics, and antimycotics. Then, the medium was replaced with Opti-MEM I (Invitrogen). The cells were transfected with 16 μg of purified cDNA of pcDNA:hIP or its mutant and 40 μL of Lipofectamine 2000 (Invitrogen). Four hours later, the medium was replaced with high-glucose Dulbecco's modified Eagle's medium containing 10% fetal bovine serum, antibiotics, and antimycotics. Approximately 48 h after transfection, the cells were harvested in ice-cold phosphate-buffered saline buffer and collected by centrifuge for further protein determination and binding assay.

Peptide Antibody Production. The three peptides corresponding to the sequences of the three extracellular loops of human IP receptor were synthesized. Each HPLC-purified peptide was coupled to keyhole-limpet haemocyanin (KLH) using glutaldehyde. Female New Zealand White rabbits were immunized with a mixture of 100 μg of each peptide−KLH conjugate in Freund's complete adjuvant. Booster immunizations with 200 μg of conjugate in Freund's incomplete adjuvant were given on days 14, 28, and 48. Blood was collected from the marginal ear vein starting 7 days after the final injection, and IgG fractions were isolated from the resulting antiserum by Na_2SO_4 precipitation and DE52-cellulose ion-exchange chromatography. The antibodies were further purified by affinity chromatography using the appropriate peptides immobilized on CNBr-activated Sepharose 4B (*24*).

Western Blot. The transfected COS-7 cells were scraped from the 10-cm plates into ice-cold PBS buffer, pH 7.4, and collected by centrifugation. After washing three times, the pellet was resuspended in a small volume of the same buffer. Each protein sample (20 μg) was separated by 10% polyacrylamide gel electrophoresis under denaturing conditions and then transferred to a nitrocellulose membrane. A band recognized by particular primary antibody was visualized with horseradish peroxidase substrate as described previously (*17*).

Ligand Binding Assay. Ligand binding assay for the IP receptor overexpressed in the COS-7 cells was performed by the method as described by Kiriyama's group (*25*). The cell pellets (200 μg protein) were incubated with 100 nM [^{3}H] iloprost in the presence or absence of 5 μM unlabeled iloprost in the 0.1-mL reaction volume with vigorous shaking at 4 °C for 2 h. The reaction was terminated by the addition of 1 mL of the cold washing buffer, and the reaction mixture was filtered through a presoaked Whatman GF/C glass filter (Whatman, Clifton, NJ) under vacuum. After washing, the radioactivity of the IP receptor-bound [^{3}H] iloprost that remained on the glass filter was counted in 4 mL of scintillation mixture using Beckman LS6800 counter (Fullerton, CA). The binding data were analyzed by the Origin 6.1 program, and each data point derived from four assay tubes was used to determine the K_d and B_{max} values by Scatchard analyses (*25*). Repetitions were from separate experiments.

cAMP Assay. The recombinant IP receptor overexpressed in the COS-7 cells was analyzed for signal transduction capability mediated by Gs coupling using a cAMP assay according to the manufacture instructions (Amersham Biosciences). The cells placed on 96-well plates at a density of 1.5×10^4 per well were cultured overnight, at 37 °C in a humidified 5% CO_2 atmosphere in high-glucose Dulbecco's modified Eagle's medium containing 10% fetal bovine serum, antibiotics, and antimycotics. Then, the medium was replaced with Opti-MEM I (Invitrogen), and the cells were transfected with 0.2 μg of purified cDNA and 0.5 μL of Lipofectamine 2000 (Invitrogen). Four hours later, the medium was replaced with high-glucose Dulbecco's modified Eagle's medium containing 10% fetal bovine serum, antibiotics, and antimycotics. After 48 h, the cells were incubated with 0.1 μM iloprost for 30 min at 37 °C. After the incubation, the medium was removed and the cells were lysed. The intracellular cAMP content of transiently transfected cells from each well of 96-well microplates was determined by Enzyme Immunoassay (EIA) using a cAMP Biotrak EIA System. Repetitions were from separate experiments.

S*tatistical Data Analyses*. Statistical analysis was carried out using the independent *t*-test in Origin 6.1 program (OriginLab, Inc., Northampton, MA). *P* values of less than or equal to 0.05 were considered to indicate a statistically significant difference.

RESULTS

Design and Synthesis of the IP iLP1 and the C-Terminal Domain of Gαs Protein for Protein−Protein Interaction. A basic residue, Arg60 in TP iLP1, is conserved in all the prostanoid receptors with Arg or Lys (*14*, Figure 1). A constrained synthetic peptide approach has recently been developed for the studies of prostanoid receptors (*26*). A peptide corresponding to the human IP iLP1 domain with a constrained N- and C-terminal distance (10−12 Å) by the addition of a homocysteine disulfide bond, based on the 7TM model of the human IP that was generated by molecular modeling using bovine rhodopsin as a template (*27*, Figure 2A), was synthesized and used for identifying the residues important to IP signaling. On the other hand, a synthetic peptide, Gαs-Ct, corresponding to the C-terminal 11 residues of the Gαs protein with an internal Tyr residue and an additional N-terminal Trp residue (providing fluorescence signal) was synthesized (Figure 2B) and used for the initial studies of its binding to the IP iLP1 peptide. In addition, synthetic unconstrained IP iLP1 and constrained TP iLP1 peptides were employed as controls for the binding studies (Figure 3).

Characterization of the Interaction of the Constrained IP iLP1 Peptide and the Gαs-Ct Peptide Using Fluorescence Spectroscopy. Fluorescence spectroscopy is a convenient approach for screening the binding of the peptide with other molecules in solution. An interaction between the constrained

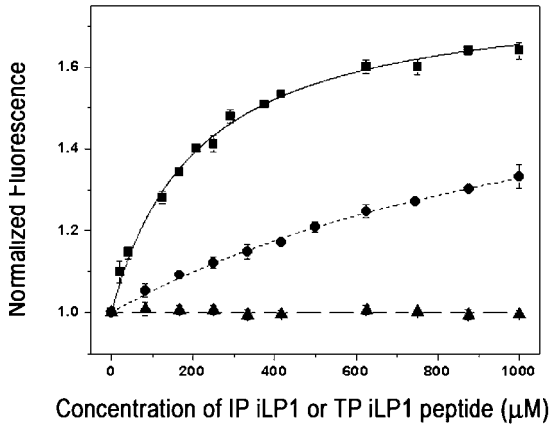

FIGURE 3: Fluorescence spectroscopic analysis for the interaction of the constrained iLP1 peptide with the Gαs-Ct peptide. The fixed amount (5 μM) of the constrained Gαs-Ct peptide was incubated with the increasing amounts (0−1000 μM) of the constrained IP iLP1 peptide (square), the unconstrained IP iLP1 peptide (circle), or the constrained TP iLP1 peptide (triangle) at room temperature. The fluorescence intensities of the mixtures were monitored at 279.6 nm for excitation and 303 nm for emission as described in Experimental Procedures. The normalized fluorescence (NF) was fitted to eq 2, and the K_d values for both of the constrained IP iLP1 peptide (204 ± 19 μM) and the unconstrained IP iLP1 peptide (1397 ± 95 μM) binding to the Gαs-Ct peptide were established. The results presented in the figure as the mean ± standard error (SE) are representative data from four assays ($n = 4$). Repetitions were from separate experiments.

TP eLP2 with its ligand, SQ29,548, has previously been identified by fluorescence spectroscopy (*18*). More recently, the interaction of the constrained IP eLP2 with its agonist, iloprost, has also been identified by the similar fluorescence spectroscopic studies (*27*). These results offer a basis to test the possible interaction of the IP iLP1 with the particular domain of Gαs protein using a synthetic peptide technique. To determine the K_d value, the fluorescence emission intensities at 303 nm for the Tyr residue were used. Figure 3 showed that the fluorescence intensity of the Gαs-Ct peptide was increased in a saturation manner as the concentration of the IP iLP1 peptide was increased, which suggested that the conformational change of the Gαs-Ct peptide may occur upon binding to the IP iLP1 peptide. By fitting the data to eq 2, we obtained a K_d value of 204 ± 19 μM for the constrained IP iLP1 peptide (Figure 3). In contrast, a much higher K_d value of 1397 ± 95 μM for the unconstrained IP iLP1 peptide was obtained, suggesting a weaker contact between the unconstrained IP iLP1 and Gαs-Ct peptide. Moreover, no significant fluorescence changes were induced upon the addition of the constrained TP iLP1 peptide to the Gαs-Ct peptide, suggesting no interaction between the two peptides (Figure 3). These results further supported that the interaction of the constrained IP iLP1 segment with the C-terminal domain of the Gαs protein could be specific. In addition, on the basis of the known factors of the fixed concentration of the Gαs-Ct peptide (5 μM) incubated with the increasing amounts of the constrained IP iLP1 peptide with a K_d value of 204 μM, the percentage of the bound form of the Gαs-Ct peptide during the titration could be calculated from [RG]/[Gαs-Ct] × 100%. When the concentrations of the IP iLP1 peptide were increased from 10 to 1000 μM, 4.6−83.0% of Gαs-Ct peptide bound to the iLP1 peptide was obtained by the calculation. Therefore, the result of our fluorescence experiment was very significant.

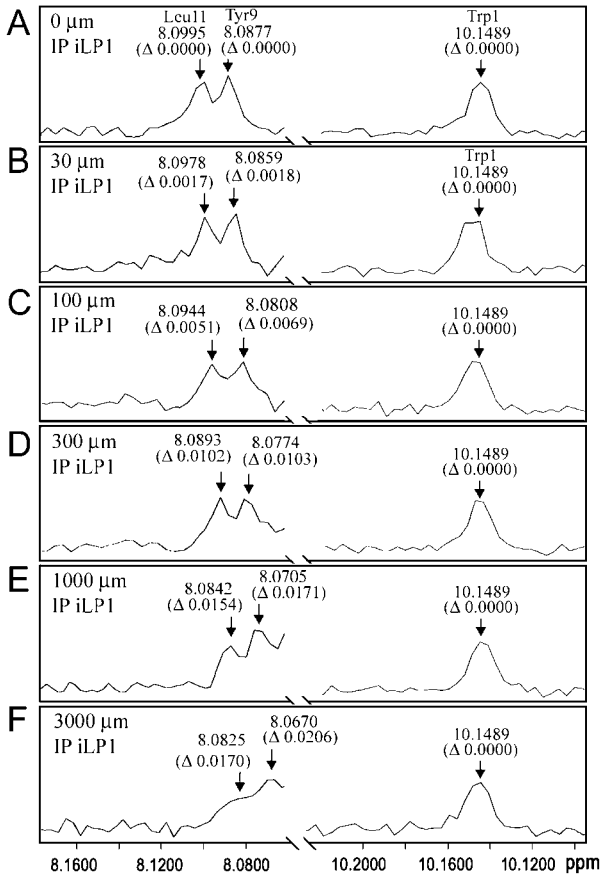

FIGURE 4: 1D ^{1}H NMR titration for the interaction of the constrained IP iLP1 peptide with the Gαs-Ct peptide. The fixed amount of the Gαs-Ct peptide (100 μM) was titrated by additions of the increasing amounts (0 μM (A), 30 μM (B), 100 μM (C), 300 μM (D), 1000 μM (E), and 3000 μM (F)) of the constrained IP iLP1 peptide. The observed chemical shifts for the NHs of Leu11, Tyr9, and indole proton of Trp1 (δ_{obs}) and their chemical shift perturbations ($\Delta\delta_{obs}$) in ppm during the titrations were shown.

Characterization of the Interaction of the Constrained IP iLP1 Peptide and the Gαs-Ct Peptide Using 1D ^{1}H NMR Spectroscopy. The titration of the fluorescence experiments have established the binding K_d and the specific binding nature of the peptides. The synthetic peptides with molecular weight of 1−2 kDa are ideal sizes for proton level characterization using high-resolution ^{1}H NMR experiments. Thus, the contact residues between the IP iLP1 and the Gαs-Ct peptides were further investigated by NMR spectroscopic studies. The titration of the binding of the IP iLP1 peptide to the Gαs-Ct peptide was monitored by 1D ^{1}H NMR spectroscopy using the additions of increasing amounts (30 ∼ 3000 μM) of the iLP1 peptide to the fixed amount (100 μM) of the Gαs-Ct peptide (Figure 4) similar to the titration studies using fluorescence technique.

The specific contact between the two peptides was supported by the observation of the proton resonance shifts of the particular residues in a concentration-dependent manner (Figure 4).Therefore, equilibrium dissociation constants (K_d) were estimated from the plots of $\Delta\delta$ of the residues in the Gαs-Ct peptide versus the increasing concentrations of the added IP iLP1 peptide. For the Gαs-Ct peptide, the shifts of the proton resonances of HNs in Tyr9

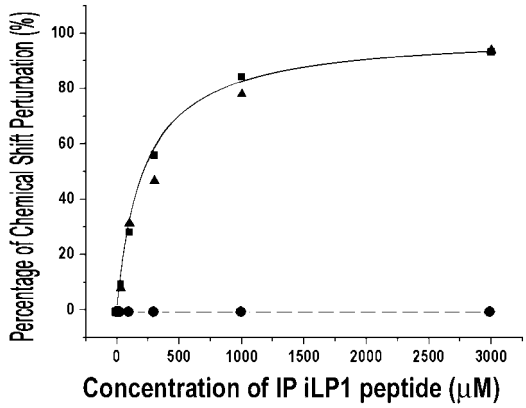

FIGURE 5: The plots of chemical shift perturbations for the NHs of Leu11 (square), Tyr9 (triangle), and indole proton of Trp1 (circle) in the Gαs-Ct peptide as described in Figure 4. The percentage of the proton chemical shift perturbation (F) shown in Figure 4 was fitted to eq 9, and the K_d value (212 μM) for the constrained IP iLP1 peptide binding to the Gαs-Ct peptide was established. The lines represent the best fitted curves.

and Leu11 could be followed throughout the titration experiments that gave a K_d value of 212 μM (Figure 5), which was very close to the K_d value observed by the fluorescence titration experiments (Figure 3). In contrast, the internal control peak of the indole proton of Trp1 residue was unchanged (Figures 4 and 5). The detailed procedures for the calculation of the K_d values were described in Experimental Procedures. The saturation-like curve of the NMR titration data in Figure 5 also shows that the interaction between the two peptides is a specific 1:1 binding as indicated by the fluorescence studies (Figure 3). During the titration, there occurred line broadening of HN of Tyr9 in the Gαs-Ct peptide due to the chemical exchange with very high concentration of the IP iLP1 peptide (Figure 4F), indicating fast exchange progressing to intermediate exchange for this proton. This provided another piece of evidence for the interaction between the two peptides in the solution. It shall also be indicated that the control experiments using either iLP1 or Gαs-Ct alone at the same highest concentration of the peptide titration did not show any chemical shift changes in ppm. This excluded the possibility of the ppm changes in the titration experiment resulting from the nonspecific peptide aggregation by itself.

Characterization of the Interaction of the IP iLP1 Peptide and the Gαs-Ct Peptide Using 2D ^{1}H NMR Spectroscopy. The interaction between the IP iLP1 peptide and the Gαs-Ct peptide was further identified by the observation of the chemical shift perturbations in the IP iLP1 peptide by comparing the 2D ^{1}H spectra, TOCSY (Figure 6), NOESY, and DQF−COSY (data not shown) of the constrained IP iLP1 peptide in the absence (Figure 6A) and presence of the Gαs-Ct peptide (Figure 6B) recorded in H_2O with 10% D_2O. The proton resonance assignments for the 2D ^{1}H NMR spectra were accomplished using the standard sequential assignment technique based on the proton chemical shifts (*18*, *28*−*30*). The assignment procedures involved the identification of the chemical shifts using the TOCSY spectrum (*31*, *32*, Figure 6) and the sequential assignment using the NOESY spectra (*33*). The complete proton resonance assignments for the constrained IP iLP1 segment (Table 1) and the Gαs-Ct peptide (Table 2) were obtained.

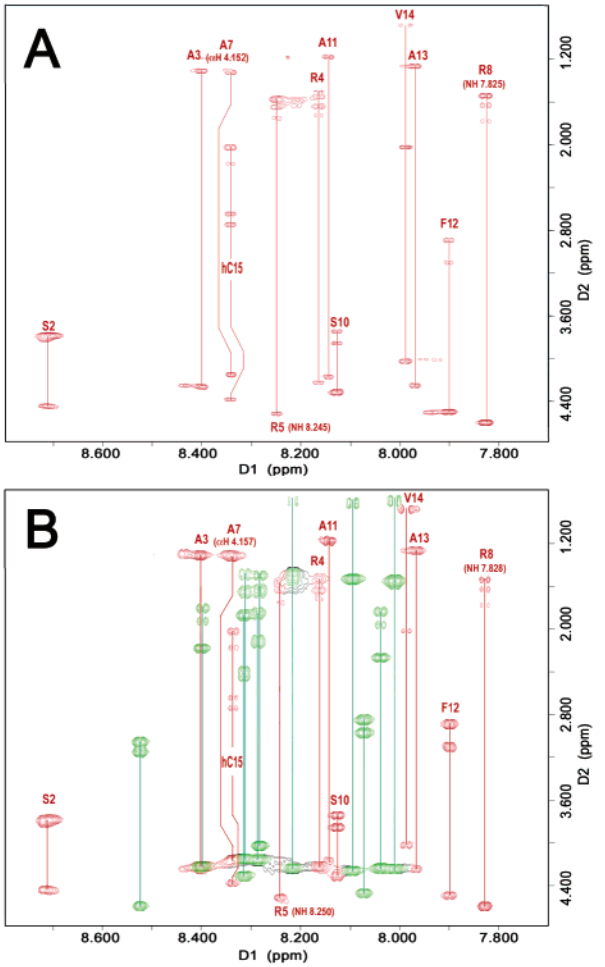

FIGURE 6: The expanded αH−NH region of the TOCSY spectra (50 ms mixing time) for the constrained IP iLP1 peptide (5.4 mM) in the absence (A) and the presence (B) of the Gαs-Ct peptide. The spectra were collected at 298 K in H_2O for the IPiLP1 peptide only (A), and for the mixture of the IPiLP1 peptide (cross-peaks in red color) and the Gαs-Ct peptide (8.4 mM, cross-peaks in green color). The chemical shift perturbations of the particular residues were represented by the ppm values in the parentheses.

Table 1: Proton Resonance Assignment (in ppm) for the Constrained IP iLP1 Peptide

residues	NH	αH	βH	γH	others
hCys1		4.09	2.25, 2.23	2.74, 2.72	
Ser2	8.71	4.45	3.81, 3.79		
Ala3	8.40	4.26	1.31		
Arg4	8.16	4.23	1.72, 1.65	1.56, 1.51	ϵH 7.09; δCH$_2$ 3.10, 3.10
Arg5	8.25	4.52	1.75, 1.64	1.59, 1.58	ϵH 7.11; δCH$_2$ 3.11, 3.11
Pro6		4.33	1.92, 1.91	2.20, 1.86	δCH$_2$ 3.72, 3.53
Ala7	8.34	4.15	1.33		
Arg8	7.82	4.60	1.76, 1.64	1.55, 1.54	ϵH 7.11; δCH$_2$ 3.14, 3.13
Pro9		4.28	1.99, 1.92	2.22, 1.87	δCH$_2$ 3.70, 3.57
Ser10	8.13	4.31	3.85, 3.75		
Ala11	8.15	4.17	1.19		
Phe12	7.90	4.50	3.10, 2.91		ϵ (3,5) 7.28; ζ (4) 7.23; δ (2,6) 7.17
Ala13	7.97	4.24	1.27		
Val14	7.99	4.02	2.02	0.89, 0.87	
hCys15	8.34	4.38	2.17, 2.03	2.75, 2.65	

Through comparison, the side chains of the residues in the IP iLP segment contacting with the Gαs-Ct were predicted by significant shifts of the resonances belonging to the particular residues. As a conclusion from both TOCSY spectrum assignments, the chemical shift perturbations

Table 2: Proton Resonance Assignment (in ppm) for the Gαs-Ct Peptide

residues	NH	αH	βH	γH	others
Trp1		4.24	3.31, 3.28		2H, 7.22; 4H, 7.46; 5H, 7.05;6H, 7.15; 7H, 7.42; indole,10.15
Gln2	8.40	4.22	1.93, 1.82	2.18, 2.18	
Arg3	8.29	4.03	1.66, 1.63	1.50, 1.50	ϵH 7.10; δCH_2 3.08
Met4	8.32	4.32	1.87, 1.86	2.45, 2.40	
His5	8.53	4.59	3.14, 3.07		2H, 7.83; 4H, 7.28
Leu6	8.22	4.24	1.48, 1.47	1.53	δCH_3 0.83, 0.78
Arg7	8.31	4.15	1.67, 1.65	1.51, 1.48	ϵH 7.08; δCH_2 3.09
Gln8	8.29	4.16	1.86, 1.85	2.12, 2.09	
Tyr9	8.09	4.48	2.96, 2.86		δ (2,6) 7.01; ϵ(3,5) 6.72
Glu10	8.04	4.25	1.95, 1.85	2.27, 2.27	
Leu11	8.10	4.27	1.53, 1.53	1.53	δCH_3 0.85, 0.80
Leu12	8.06	4.24	1.56, 1.56	1.56	δCH_3 0.83, 0.78

(0.003−0.006 ppm) were localized at NH in Arg42, αH in Ala44, and NH and δH in Arg45 of the IP iLP1 segment, which were induced by the interaction with the Gαs-Ct peptide (Figure 6, Table 3). In contrast, the protons in other residues of the IP iLP1 were not significantly affected by the presence of the Gαs-Ct peptide. These results suggested that these residues of the IP iLP1 were involved in the interaction with the Gαs-Ct peptide in the solution and implied that these residues in the IP receptor protein could be the target residues involved in the receptor-Gαs coupling in the receptor signaling. It is particularly interesting that these data provided the first clues suggesting that multiple residues surrounding the Arg45 in the IP iLP1 may be involved in the receptor signaling.

The interaction of the IP iLP1 peptide with the Gαs-Ct peptide was further confirmed by the high-resolution 2D ^{1}H NMR spectroscopy using the comparison of the complete 2D spectrum assignments for the Gαs-Ct peptide in the absence (Figure 7A, Table 4) and presence (Figure 7B) of the IP iLP1 peptide. The significant chemical shift perturbations (0.003−0.012 ppm) of the proton resonances of the residues of Tyr9, Glu10, Leu11, and Leu12 in the Gαs-Ct peptide were clearly observed (Figure 7, Table 4). The chemical shift perturbations of the Gαs-Ct peptide upon interaction with the IPiLP1 peptide observed in the NMR experiments is consistent with the early observation that the conformation of the C-terminal of Gt protein α-subunit was changed upon interaction with the rhodopsin (*13*).

Evaluation of the Conserved Arg45 in the IP iLP1 Important to the Receptor Signaling. Arg45 in the IP iLP1 is the corresponding residue to Arg60 in the TP iLP1 that has been identified as a key residue important to the TP signaling through Gαq coupling. As described above, Arg45 is one of the residues contacted with the Gαs-Ct peptide by

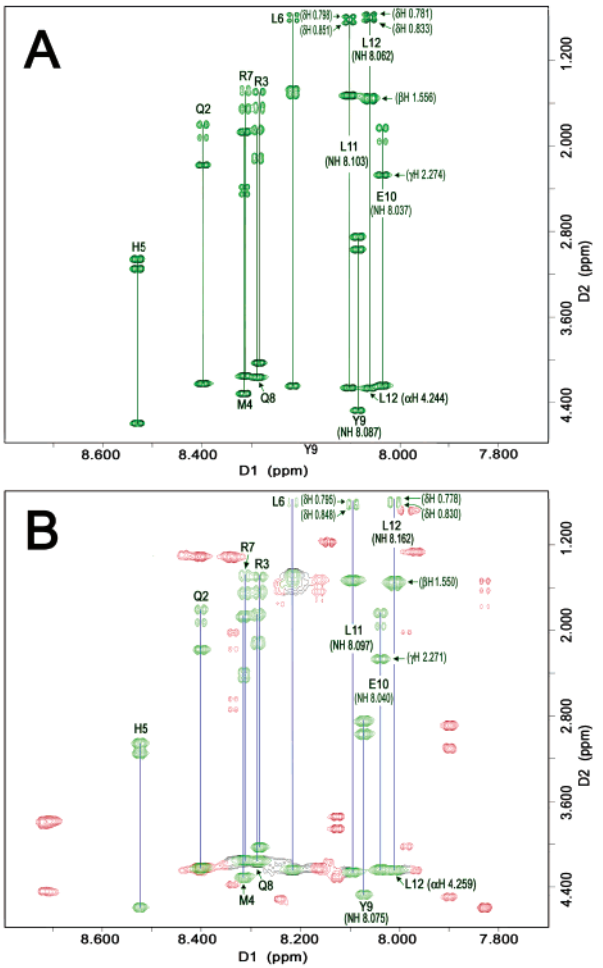

FIGURE 7: The expanded αH−NH region of the TOCSY spectra (50 ms mixing time) for the Gαs-Ct peptide in the absence (A) and presence (B) of the IPiLP1 peptide. The spectra were collected at 298 K in H_2O for the Gαs-Ct peptide only (8.4 mM, A), or the mixture of the Gαs-Ct peptide (cross-peaks in red color) and the constrained IP iLP1 peptide (5.4 mM, cross-peaks in green color). The chemical shift perturbations of the particular residues were represented by the ppm values in the parentheses.

the NMR studies using the IP iLP1 fragment. Thus, it is the most important target to be considered as a residue involved in the receptor signaling through Gαs. To test this hypothesis, four recombinant human IP receptors with a point mutation of Arg45Leu, Arg45Lys, Arg45Glu, and Arg45Gln were generated. The correct point mutation was confirmed by the DNA sequencing, and the overexpression of the mutants in the COS-7 cells was confirmed by Western blot analysis (Figure 8A). The binding of the recombinant receptors to its ligand was then performed using [^{3}H] iloprost. Unlabeled (cold) iloprost (5 μM) was also used as a competitive ligand

Table 3: The Shifts (in ppm) of the Proton Resonances in TOCSY Spectra of the Particular Residues of the Constrained IP iLP1 Peptide (5.4 mM) Induced by the Addition of the Gαs-Ct Peptide (8.4 mM)

residues in IP iLP1 peptide	corresponding resides in IP receptor	proton	proton chemical shifts of IP iLP1 in the absence of Gαs-Ct peptide	proton chemical shifts of IP iLP1 in the presence of Gαs-Ct peptide	chemical shift perturbations
Arg5	Arg-42	NH	8.250	8.245	0.005
Ala7	Ala-44	αH	4.152	4.157	0.005
Arg8	Arg-45	NH	7.825	7.828	0.003
		δH	3.131	3.137	0.006
		δH	3.140	3.146	0.006

Table 4: The Shifts (in ppm) of the Proton Resonances in TOCSY Spectra of the Particular Residues of the Gαs-Ct Peptide (8.4 mM) Induced by the Addition of the Constrained IP iLP1 Peptide (5.4 mM)

residues in Gαs-Ct	corresponding resides in Gαs protein	proton	proton chemical shifts of Gαs-Ct: in the absence of IP iLP1 peptide	proton chemical shifts of Gαs-Ct: in the presence of IP iLP1 peptide	chemical shift perturbations
Tyr9	Tyr391	NH	8.087	8.075	0.012
Glu10	Glu392	NH	8.037	8.040	0.003
		γH	2.274	2.271	0.003
Leu11	Leu393	NH	8.103	8.097	0.006
		δH	0.851	0.848	0.003
		δH	0.798	0.795	0.003
Leu12	Leu394	NH	8.062	8.012	0.050
		αH	4.244	4.259	0.015
		βH	1.556	1.550	0.006
		δH	0.833	0.830	0.003
		δH	0.781	0.778	0.003

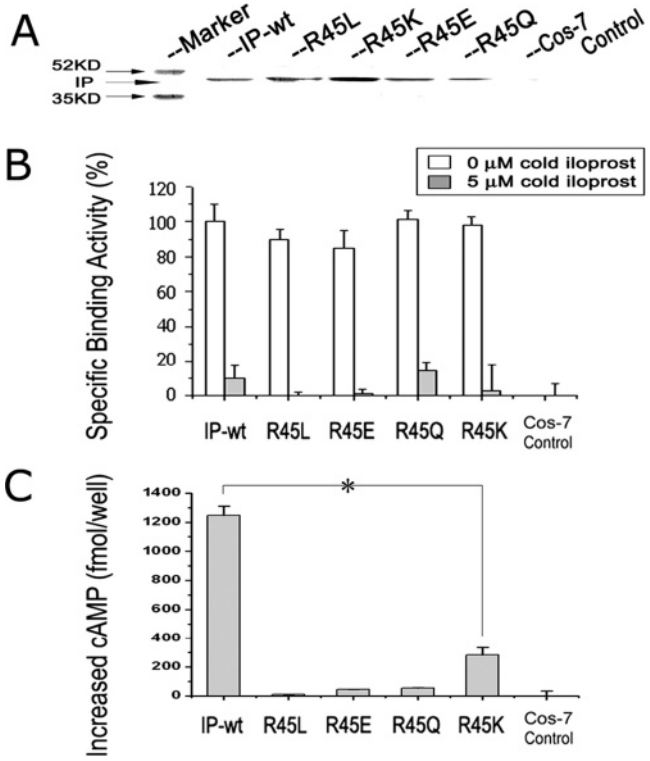

FIGURE 8: Functional properties of the wild-type (IP-wt) and mutant IP receptors at the site of Arg45 overexpressed in COS-7 cells. (A) Western blot of the recombinant receptors of IP-wt and the Arg45 mutants. (B) Binding of the recombinant IP receptors to 100 nM [^{3}H] iloprost (added 20 000 cpm, open bars). Unlabeled iloprost (5 μM) was used for competitive binding (shaded bars). One hundred persent of the specific binding is 1200 cpm. The results were the averages from three experiments. (C) The intracellular cAMP production of transiently transfected cells in 96-well microplates, stimulated by iloprost, was determined by EIA assay as described in Experimental Procedures. The results presented in the figure as the mean ± standard error (SE) are representative data from four independent experiments ($n = 4$). Repetitions were from separate experiments, and the p value for that with the decreased activity was shown (*, $p \leq 0.05$).

to show the specific binding. The binding of the four mutants to iloprost was the same as the wild-type (Figure 8B), indicating that the mutants of Arg45 to Leu, Lys, Glu, or Gln did not affect receptor folding nor alter the ligand-binding site in general. However, in comparison with the wild-type, the mutants of Arg45Leu, Arg45Glu, and Arg45Gln completely lost their cAMP production activity, which is a signaling indicator of Gαs coupling (Figure 8C), indicating the positive charge of Arg45 is important to the signaling. In addition, the mutant of Arg45Lys could only recover about 25% of the signaling activity, indicating the other factors beside the positive charge are also important to Gαs coupling. These results provided the first experimental evidence which showed that the conserved Arg45 at the IP iLP1 is similar to the Arg60 at the TP iLP1 in its importance to receptor signaling through different G protein coupling systems. It also supported the NMR experimental prediction that Arg45 is involved in IP receptor signaling.

Confirmation of the NMR Experiment-Based Prediction for the Other Residues in the IP iLP1 Involved in Gαs Protein Coupling Using Recombinant IP Receptors. The mutation at Arg45 has clearly indicated that the NMR experiment provided useful information for the prediction of the particular residue important to the receptor signaling. The NMR experiments have also predicted other residues surrounding Arg45, including Arg42 and Ala44 in the IP iLP1, are important to the Gαs-Ct contacts (Table 2). To test whether the surrounding results are also important to the receptor signaling at a protein level, a series of recombinant proteins of the human IP receptor with point mutation from the residues 39−51, covering all of the putative iLP1 region except for the Arg45, were constructed by the PCR mutagenesis approach. These residues were replaced with Gly one by one to eliminate the side-chain functions and slightly change the local conformation by the phi-psi angles. Each point mutation was confirmed by DNA sequencing. After transfection of the cDNA into COS-7 cells, the expression levels of the IP receptor mutants similar to the wild-type were observed in Western blot (Figure 9A). The binding of the recombinant receptors to its ligand was then performed using [^{3}H] iloprost as described above. All of the mutations retained ligand-binding activities similar to the wild-type (Figure 9B), suggesting that each of them has the same correct protein folding in the cell membrane as that of the wild-type. However, the recombinant IP receptors with point mutations at residues 42−48 (including Arg45Leu mutant) to Gly lost 70−100% of their ability to produce cAMP through the Gαs coupling (Figure 9C), which include the residues predicted from the NMR experiments. The EC_{50} for the wild-type human IP receptor expressed in COS-7 cells was about 0.2 nM of iloprost (*34*). The EC_{50} values of iloprost for the mutants at residues 42−48 were expected to

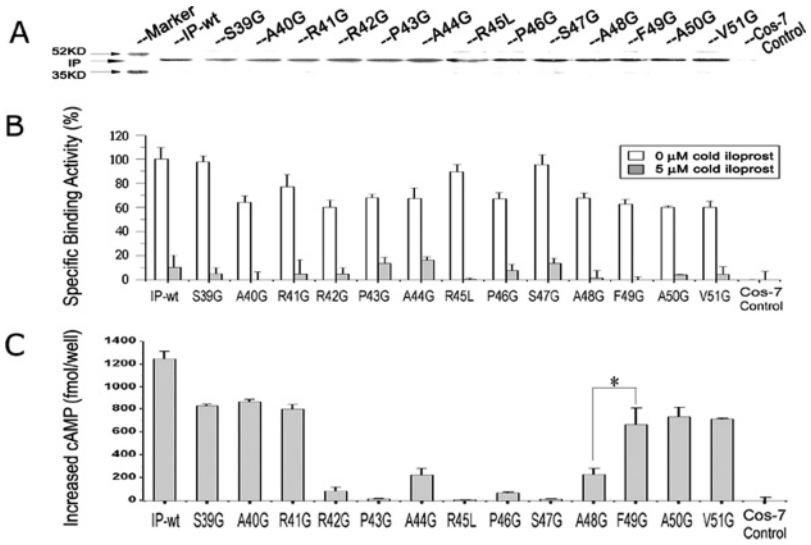

FIGURE 9: Functional properties of the wild-type (IP-wt) and 13 IP receptor mutants overexpressed in COS-7 cells. (A) Western blot of the recombinant IP receptors. (B) Binding of the recombinant IP receptors to 100 nM [^{3}H] iloprost (open bars). Unlabeled iloprost (5 μM) was used for competitive binding (shaded bars). (C) The intracellular cAMP production of transiently transfected cells in 96-well microplates, stimulated by iloprost, was determined by EIA assay as described in Experimental Procedures. The results presented in the figure as the mean ± SE are representative data from four independent experiments ($n = 4$). Repetitions were from separate experiments, and the p value for that with the decreased activity was shown (*, $p \leq 0.05$).

be over 100 nM, because under the stimulation of 100 nM of iloprost, the assay showed that the cAMP production of these mutants decreased significantly (more than 70%) from that of the wild-type. In comparison, the receptor with point mutation at residues 39−41 and 49−51 did not significantly lose the function of the cAMP production. These results revealed that the residues 42−48 including the residues of Arg42 and Ala44 predicted by the NMR experiments are involved in the IP receptor signaling through Gαs protein coupling. Thus, the NMR peptide studies could be a powerful tool to provide an initial clue in locating the target residues and region for functional characterization of the protein. It shall be indicated that some residues in IP iLP1, important to the IP signaling found in mutagenesis studies, were not initially observed in the NMR peptide studies. This demonstrated that the peptide NMR experiment might not necessarily be able to localize all of the important residues in the intact protein. The combination of the NMR peptide study and protein mutagenesis should be more reliable.

Specificity of the Important Residues in the IP Signaling. That the mutation of Arg45 to Lys with a similar positively charged side chain could not completely restore the IP receptor signaling activity has indicated that other chemical and structural features such as conformation, size, and different charge surface of the Arg45 side chain are also important to the specific Gαs coupling. This observation is similar to that of the Arg60 residue at the TP iLP1, which couples to Gαq (*17*). To further test the specificities of the other conserved residues in the IP iLP1 important to the IP signaling, the residues including Ser47 and Ala48 were replaced with the corresponding similar residues of Thr in the EP4 iLP1 and Leu in the DP iLP1, respectively (Figure 1). Thus, the two mutants of Ser47Thr and Ala48Leu of the IP receptor were further created by the PCR mutagenesis and expressed in the COS-7 cells (Figure 10A) for their functional tests. In addition, three other mutants of Pro46Ala, Ser47Ala, and Ala48Val of the IP receptor were also generated and expressed in COS-7 cells for detailed functional analysis of the side chains (Figure 10A). All of those mutants showed binding to iloprost similar to or slightly less

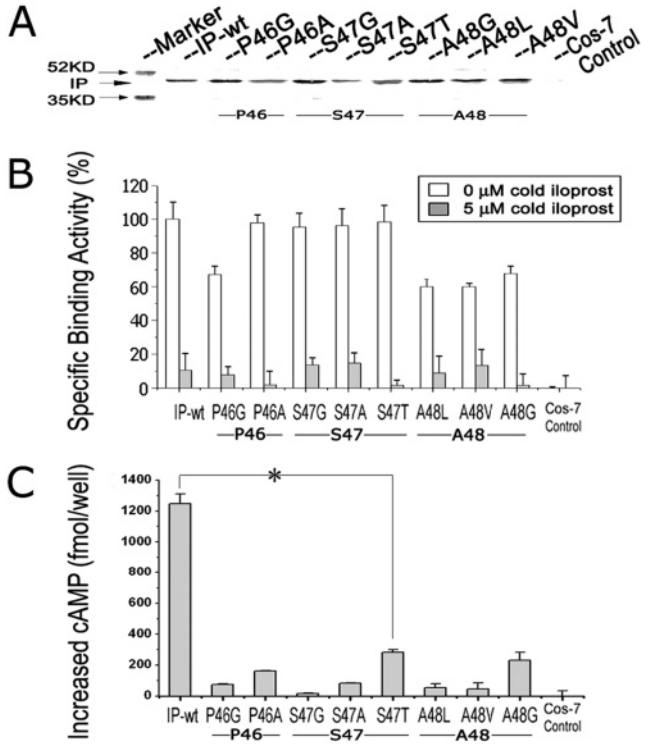

FIGURE 10: Functional properties of the wild-type and the IP receptor mutants at the sites of Pro46, Ser47, and Ala48 overexpressed in COS-7 cells. (A) Western blot of the recombinant IP receptors. (B) Binding of the recombinant IP receptors to 100 nM [^{3}H] iloprost (open bars). Unlabeled iloprost (5 μM) was used for competitive binding (shaded bars). (C) The intracellular cAMP production of transiently transfected cells in one well of 96-well microplates, stimulated by iloprost, was determined by EIA assay as described in Experimental Procedures. The results presented in the figure as the mean ± SE are representative data from four independent experiments ($n = 4$). Repetitions were from separate experiments, and the p value for that with the decreased activity was shown (*, $p \leq 0.05$).

Table 5: Binding, Expression, and Activation of the Human Prostacyclin Receptor and Its Mutants[a]

	binding of iloprost		expression of the IP receptor		cAMP production stimulated by iloprost	
IP receptor	K_d (nM)	percentage (%)	B_{max} (fmol/mg)	percentage (%)	cAMP (fmol/1.5 × 10^4 cells)	percentage (%)
wild-type	12.8 ± 5.3	100	128 ± 18	100	1248 ± 62* #	100
mutant R42G	12.2 ± 2.4	95	114 ± 9	89	87 ± 32	7
mutant P43G	22.9 ± 3.3	179	92 ± 5	72	21 ± 5	2
mutant A44G	13.4 ± 2.4	105	62 ± 3	48	227 ± 92#	18
mutant R45L	12.4 ± 5.3	97	64 ± 8	50	10 ± 3	1
mutant P46G	11.4 ±2.2	89	80 ± 4	63	75 ± 4	6
mutant S47G	12.5 ± 3.0	95	75 ± 8	58	17 ± 7	1
mutant A48G	6.2 ± 3.3	51	81 ± 6	64	230 ± 51*	18

[a] The results presented in figures as the mean ± standard error (SE) are representative data from four independent experiments ($n = 4$). Repetitions were from separate experiments, and the p values for those with decreased activity are shown (*, $p \leq 0.05$; #, $p \leq 0.05$).

than the wild-type IP receptor (Figure 10B), but their cAMP production activities through Gαs coupling were significantly impaired (Figure 10C). These results indicated that the chemical and structural properties of the side chains of those residues are also highly specific and similar to Arg45 in the IP iLP1. Maintaining the conformation with the correct side chains of the residues is the basis to maintain the active signaling activity for the IP receptor.

Effects of the Mutations in the IP iLP1 Region on the Ligand Binding Affinity in the Extracellular Domains. To test whether the impairment of the signing of the IP mutations in the iLP1 region affect their ligand binding affinity that occurred in the extracellular domains, kinetic studies of the ligand bindings for the mutants without signaling activities were performed by titration experiments. The specific binding was obtained by the subtraction of the total binding from the nonspecific binding in the presence of the cold iloprost (Figure 11). The seven mutants important to IP signaling showed very similar K_d values when compared to the wild-type (Figure 11 and Table 5). These results strongly indicate that the mutations at the iLP1 region have no significant effect on receptor ligand binding, and the identified residues in the iLP1 region important to receptor signaling are indeed involved in the G protein coupling in the intracellular domains and irrelevant to ligand binding occurring in the extracellular and/or transmembrane domains.

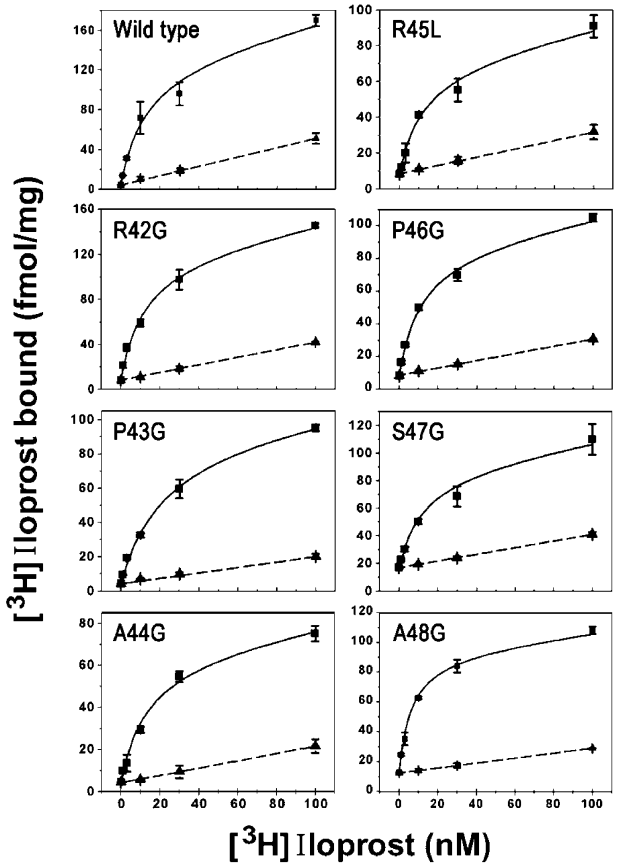

FIGURE 11: Kinetic properties of [^{3}H] iloprost binding to the recombinant IP receptors expressed in COS-7 cells. The cell membrane protein prepared from COS-7 cells that transiently expressed the wild-type or the mutants of the IP receptor was incubated with the increasing concentration of the [^{3}H] iloprost in the absence (square) or presence (triangle) of 500-fold excess of a unlabeled iloprost. The results presented in the figure as the mean ± SE are representative data from four independent experiments ($n = 4$). Repetitions were from separate experiments.

DISCUSSION

Eight prostanoid receptors including IP and TP have been cloned for a decade, but little information is available for their specific ligand recognition and signaling in structural terms. However, the difficulty of the crystallization of the membrane-bound GPCRs makes obtaining crystal structures for the prostanoid receptors unlikely to occur immediately. NMR spectroscopy offers an alternative way to solve the peptide and protein structures in solution. However, the high-resolution NMR technique for the sizes of the membrane-bound prostanoid receptors (30 kD and up) can be very difficult because of the slow tumbling of the larger molecules. Thus, it has limited the use of the NMR technique for the structural and functional characterization of the prostanoid receptors directly using the membrane proteins. Recently, several novel NMR spectroscopic techniques have been developed to determine the interaction between protein and ligand (*35*−*47*), as well as peptide and peptide, which include the transferred NOE effects (*48*−*54*) and the chemical shift perturbations (*55*−*59*). However, to identify the residues important to the protein−protein interaction on the membrane proteins in structural terms is still a big challenge for the high-resolution NMR spectroscopy. On the other hand, site-directed mutagenesis is used for screening the functional residues of the protein. But, without structural support, the one-by-one mutagenesis is not time efficient. In addition, the mutation result might not directly apply to the understanding of the structure/function relationship at molecular and atomic levels because the mutation may cause post-translational changes of the proteins, such as protein folding, glycosylation, membrane incorporation, and signaling. To utilize the advantages of high-resolution NMR spectroscopy,

for the determination of the solution structure of peptide at a proton level, and site-directed mutagenesis, for the identification of the protein function at single residue level, the combination of the two approaches into a single system may enable enlargement of the scope and enhancement of the powers of either approach individually. On the basis of this concept, we have introduced a strategy to characterize the structure/function relationship of prostanoid receptors and synthases using a system connecting the NMR spectroscopy for peptide and mutagenesis for protein together. This strategy has enhanced our knowledge in the understanding of the structure/function relationship of the TP receptor interacting with its ligand in extracellular domains and interacting with Gαq in the first intracellular loop (*17*). The strategy was also used to understand the mechanism of prostacyclin synthase contacting with the endoplasmic reticulum membrane and docking with its substrate (*60*). In the current studies, the developed strategy using NMR spectroscopy combined with protein mutagenesis was further used to identify the residues in the IP iLP1 important to the receptor signaling through Gαs coupling. The results have provided evidences allowing the localization of important residues. It should also be suitable to characterize the structure and function relationship for the other prostanoid receptors.

Many attempts have been made to find a G protein coupling site on the intracellular domains of the GPCRs. The second (iLP2) and third (iLP3) intracellular loops and the C-terminal domain of GPCRs involving their G protein coupling have been identified in different GPCRs (*61*−*64*). Generally, iLP2s and iLP3s are important players in specificity and/or efficiency of G protein activity in some GPCRs, while iLP1s are thought to be relatively unimportant (*64*). However, recent studies provide substantial evidences demonstrating that the iLP1s in GPCRs are also involved in the receptor signaling through different G protein coupling (*65*−*78*). The detailed molecular mechanism of the iLP1s of the prostanoid receptors involved in their signaling has previously been poorly addressed until our recent structural and functional characterization of the TP iLP1 (*14*). Instead of testing the single residue (Arg60) crucial to the TP receptor signaling, the studies described in this paper expanded one step further to characterize the profile of the residues in the entire putative iLP1 region involved in the signaling and explore the molecular mechanism of the signaling through the interaction of the IP iLP1 and the C-terminal of the Gαs protein. Thus, the conclusion is more valuable than our previous studies.

The profile of the important residues in the IP iLP1 with a continuous seven residues from 42 to 48 provided important information for further understanding on the molecular basis: (1) The iLP1 contains an epitope crucial to the receptor signaling through Gαs coupling, not just the conserved Arg45. (2) The epitope is likely to be involved in contact with the Gαs, supported by the observation of the interaction of the constrained IP iLP1 peptide with the Gαs-Ct peptide in the fluorescence and NMR spectroscopic studies (Figures 3−7 and Tables 3 and 4). (3) The side chains of the continuous seven residues are in a loop configuration allowing orientation to different directions, which is favorable to be predicted for the intermolecular contact instead of intramolecular interaction. (4) The conservation of similar residues for the seven residues in the iLP1s of other prostanoid receptors compared to the IP iLP1 (Figure 1) implies that a similar epitope is present in the iLP1s of the other prostanoid receptors having similar functions in their signaling through different G protein coupling systems. (5) Replacement of the Lys for Arg45, Thr for Ser47, and Leu for Ala48 in the IP iLP1 could not completely restore the receptor signaling activity, indicating that, besides the chemical properties, the conformation of the side chains of the residues may also participate in the protein−protein interaction.

Some residues important for IP coupling may not be detected in a NMR experiment. One of the reasons is that the chemical shift perturbation tends to emphasize shifts of large, solvent-exposed residues (Tyr, Lys, Arg, His) and underemphasized interactions with buried or smaller residues (Gly, Ala) (*79*). The other reason is that our NMR model only employs the C-terminal region of Gαs, but we cannot exclude the possibility that other regions on Gαs or the G$\beta\gamma$ dimer may also be involved in receptor contact (*80*).

It has been reported that the human IP receptor could also couple to the Gαq protein (*3*). This phenomenon is observed in many cell lines, including CHO cells (*81*) and HEK 293 cells (*82*). How does the IP receptor communicate to different G proteins at residue level? This is a very interesting question and has not yet been addressed clearly. Our recombinant human IP receptor mutants can be used as a tool to study the mechanisms of the Gαs/Gαq coupling systems for the receptor. For example, to test whether the Gαq coupling in the IP receptor is independent from the Gαs coupling, the recombinant IP receptor with a single mutation (such as Arg45Lys, Ser47Thr, or Ala48Leu mutant) impairing the cAMP production activity through Gαs coupling can be used to test the ability of in increasing the intracellular calcium level through Gαq coupling. Independent coupling of human IP to Gαq can be predicted if the mutant retained the ability to activate the calcium mobilization. However, if the mutant also lost the Gαq coupling activity, this would suggest that the Gαq coupling is dependent on the Gαs.

ACKNOWLEDGMENT

We thank Dr. Xiaolian Gao and Dr. Xia Youlin in the Chemistry Department at The University of Houston, TX, for access to the NMR facility and providing valuable advice on taking the NMR spectra. We also thank Lori Jenkins, Nancy Fernandez, and Sam Li for the manuscript preparation assistance.

REFERENCES

1. Boie, Y., Rushmore, T. H., Darmon-Goodwin, A., Grygorczyk, R., Slipetz, D. M., Metters, K. M., and Abramovitz, M. (1994) Cloning and expression of a cDNA for the human prostanoid IP receptor, *J. Biol. Chem. 269*, 12173−12178.
2. Wise, H. (2003) Multiple signalling options for prostacyclin, *Acta Pharmacol. Sin. 24*, 625−630.
3. Lawler, O. A., Miggin, S. M., and Kinsella, B. T. (2001) Protein kinase A-mediated phosphorylation of serine 357 of the mouse prostacyclin receptor regulates its coupling to G(s)-, to G(i)-, and to G(q)-coupled effector signaling, *J. Biol. Chem. 276*, 33596−33607.
4. Rasenick, M. M., Watanabe, M., Lazarevic, M. B., Hatta, S., and Hamm, H. E. (1994) Synthetic peptides as probes for G protein function. Carboxyl-terminal G alpha s peptides mimic Gs and

evoke high affinity agonist binding to beta-adrenergic receptors, *J. Biol. Chem. 269*, 21519−21525.
5. Lichtarge, O., Bourne, H. R., and Cohen, F. E. (1996) Evolutionarily conserved Galphabetagamma binding surfaces support a model of the G protein−receptor complex, *Proc. Natl. Acad. Sci. U.S.A. 93*, 7507−7511.
6. Onrust, R., Herzmark, P., Chi, P., Garcia, P. D., Lichtarge, O., Kingsley, C., and Bourne, H. R. (1997) Receptor and betagamma binding sites in the alpha subunit of the retinal G protein transducin, *Science 275*, 381−384.
7. Masters, S. B., Sullivan, K. A., Miller, R. T., Beiderman, B., Lopez, N. G., Ramachandran, J., and Bourne, H. R. (1988) Carboxyl terminal domain of Gs alpha specifies coupling of receptors to stimulation of adenylyl cyclase, *Science 241*, 448−451.
8. Feldman, D. S., Zamah, A. M., Pierce, K. L., Miller, W. E., Kelly, F., Rapacciuolo, A., Rockman, H. A., Koch, W. J., and Luttrell, L. M. (2002) Selective inhibition of heterotrimeric Gs signaling. Targeting the receptor−G protein interface using a peptide minigene encoding the Galpha(s) carboxyl terminus, *J. Biol. Chem. 277*, 28631−28640.
9. Gilchrist, A., Bunemann, M., Li, A., Hosey, M. M., and Hamm, H. E. (1999) Selective inhibition of heterotrimeric Gs signaling. Targeting the receptor−G protein interface using a peptide minigene encoding the Galpha(s) carboxyl terminus, *J. Biol. Chem. 274*, 6610−6616.
10. Drew, J. E., Barrett, P., Conway, S., Delagrange, P., and Morgan, P. J. (2002) Differential coupling of the extreme C-terminus of G protein alpha subunits to the G protein-coupled melatonin receptors, *Biochim. Biophys. Acta 1592*, 185−192.
11. Gilchrist, A., Vanhauwe, J. F., Li, A., Thomas, T. O., Voyno-Yasenetskaya, T., and Hamm, H. E. (2001) G alpha minigenes expressing C-terminal peptides serve as specific inhibitors of thrombin-mediated endothelial activation, *J. Biol. Chem. 276*, 25672−25679.
12. Koenig, B. W., Kontaxis, G., Mitchell, D. C., Louis, J. M., Litman, B. J., and Bax, A. (2002) Structure and orientation of a G protein fragment in the receptor bound state from residual dipolar couplings, *J. Mol. Biol. 322*, 441−461.
13. Kisselev, O. G., Kao, J., Ponder, J. W., Fann, Y. C., Gautam, N., and Marshall, G. R. (1998) Light-activated rhodopsin induces structural binding motif in G protein alpha subunit, *Proc. Natl. Acad. Sci. U.S.A. 95*, 4270−4275.
14. Hayes, J. S., Lawler, O. A., Walsh, M. T., and Kinsella, B. T. (1999) The prostacyclin receptor is isoprenylated. Isoprenylation is required for efficient receptor-effector coupling, *J. Biol. Chem. 274*, 23707−23718.
15. Wise H. (1999) Characterization of chimeric prostacyclin/prostaglandin D(2) receptors, *Eur. J. Pharmacol. 386*, 89−96.
16. Hirata, T., Kakizuka, A., Ushikubi, F., Fuse, I., Okuma, M., and Narumiya, S. (1994) Arg60 to Leu mutation of the human thromboxane A2 receptor in a dominantly inherited bleeding disorder, *J. Clin. Invest. 94*, 1662−1667.
17. Geng, L., Wu, J., So, S. P., Huang, G., and Ruan, K. H. (2004) Structural and functional characterization of the first intracellular loop of human thromboxane A2 receptor, *Arch. Biochem. Biophys. 423*, 253−265.
18. So, S. P., Wu, J., Huang, G., Huang, A., Li, D., and Ruan, K. H. (2003) Identification of residues important for ligand binding of thromboxane A2 receptor in the second extracellular loop using the NMR experiment-guided mutagenesis approach, *J. Biol. Chem. 278*, 10922−10927.
19. Wu, J., So, S. P., and Ruan, K. H. (2003) Solution structure of the third extracellular loop of human thromboxane A2 receptor, *Arch. Biochem. Biophys. 414*, 287−293.
20. Lacourciere, K. A., Stivers, J. T., Marino, J. P. (2000) Mechanism of neomycin and Rev peptide binding to the Rev responsive element of HIV-1 as determined by fluorescence and NMR spectroscopy, *Biochemistry 39*, 5630−5641.
21. Wüthrich, K. (1986) *NMR of Proteins and Nucleic Acids*, Wiley, New York.
22. Kim, S., Cullis D. N., Feig, L. A., and Baleja, J. D. (2001) Solution structure of the Reps1 EH domain and characterization of its binding to NPF target sequences, *Biochemistry 40*, 6776−6785.
23. Sanger, F., Nicklen, S., and Coulson, A. R. (1977) DNA sequencing with chain-terminating inhibitors, *Proc. Natl. Acad. Sci. U.S.A. 74*, 5463−5467.
24. Deng, H., Huang, A., So, S. P., Lin, Y. Z., and Ruan, K. H. (2002) Substrate access channel topology in membrane-bound prostacyclin synthase, *Biochem J. 362*, 545−551.
25. Kiriyama, M., Ushikubi, F., Kobayashi, T., Hirata, M., Sugimoto, Y., Narumiya, S. (1997) Ligand binding specificities of the eight types and subtypes of the mouse prostanoid receptors expressed in Chinese hamster ovary cells, *Br. J. Pharmacol. 122*, 217−224.
26. Ruan, K. H. (2004) High-resolution nuclear magnetic resonance spectroscopy-guided mutagenesis for characterization of membrane-bound proteins: experimental designs and applications, *Spectroscopy 18*, 13−29.
27. Ruan, K. H., Wu, J., So, S. P., and Jenkins, L. A. (2003) Evidence of the residues involved in ligand recognition in the second extracellular loop of the prostacyclin receptor characterized by high resolution 2D NMR techniques, *Arch. Biochem. Biophys. 418*, 25−33.
28. Englander, S. W., and Wand, A. J. (1987) Main-chain-directed strategy for the assignment of 1H NMR spectra of proteins, *Biochemistry 26*, 5953−5958.
29. Chazin, W. J., Rance, M., and Wright, P. E. (1988) Complete assignment of the 1H nuclear magnetic resonance spectrum of French bean plastocyanin. Application of an integrated approach to spin system identification in proteins, *J. Mol. Biol. 202*, 603−622.
30. Basus, V. J. (1989) Proton nuclear magnetic resonance assignments, *Methods Enzymol. 177*, 132−149.
31. Braunschweiler, L., and Ernst, R. R. (1983) Coherence transfer by isotropic mixing: application to proton correlation spectroscopy, *J. Magn. Reson. 53*, 521−528.
32. Bax, A., and Drobny G. (1985) Optimization of two-dimensional homonuclear relayed coherence transfer NMR spectroscopy. *J. Magn. Reson. 61*, 306−320.
33. Jeener, J., Meier, B. H., Bachmann, P., and Ernst, R. R. (1979) Investigation of exchange process by two-dimensional NMR spectroscopy, *J. Chem. Phys. 71*, 4546−4553.
34. Nakagawa, O., Tanaka, I., Usui, T., Harada, M., Sasaki, Y., Itoh, H., Yoshimasa, T., Namba, T., Narumiya, S., Nakao, K. (1994) Molecular cloning of human prostacyclin receptor cDNA and its gene expression in the cardiovascular system, *Circulation 90* (4), 1643−1647.
35. Diercks, T., Coles, M., and Kessler, H. (2001) Applications of NMR in drug discovery, *Curr. Opin. Chem. Biol. 5*, 285−291.
36. Shapiro, M. (2001) Applications of NMR screening in the pharmaceutical industry, *Farmaco 56*, 141−143.
37. Craik, D. J., and Scanlon, M. J. (2000) Pharmaceutical applications of NMR, *Annu. Rep. NMR Spectrosc. 42*, 115−174.
38. Fry, D. C., and Emerson, S. D. (2000) Applications of biomolecular NMR to drug discovery, *Drug Des. Discovery 17*, 13−33.
39. Roberts, G. C. (2000) Applications of NMR in drug discovery, *Drug Discovery Today 5*, 230−240.
40. Ghose, A. K., Viswanadhan, V. N., and Wedoloski, J. J. (1999) A knowledge-based approach in designing combinatorial or medicinal chemistry libraries for drug discovery. 1. A qualitative and quantitative characterization of known drug databases, *ACS Symp. Ser. 719*, 226−238.
41. Hajduk, P. J., Meadows, R. P., and Fesik, S. W. (1999) NMR-based screening in drug discovery, *Q. Rev. Biophys. 32*, 211−240.
42. Moore, J. M. (1999) NMR techniques for characterization of ligand binding: utility for lead generation and optimization in drug discovery, *Biopolymers 51*, 221−243.
43. Moore. J. M. (1999) NMR screening in drug discovery, *Curr. Opin. Biotechnol. 10*, 54−58.
44. Shapiro, M. J., and Gounarides, J. S. (1999) NMR methods utilized in combinatorial chemistry research. Progress in nuclear magnetic resonance spectroscopy, *Prog. Nucl. Magn. Reson. Spectrosc. 35*, 153−200.
45. Shapiro, M. J., and Wareing, J. R. (1999) High-resolution NMR for screening ligand/protein binding, *Curr. Opin. Drug Discovery Dev. 2*, 396−400.
46. Schriemer, D. C., and Hindsgaul, O. (1998) "Deconvolution approaches in screening compound mixtures" combinatorial chemistry and high throughput screening, *Comb. Chem. High Throughput Screening* 1, 155−170.
47. Hajduk, P. J., Meadows, R. P., and Fesik, S. W. (1997) Discovering high-affinity ligands for proteins, *Science 278*, 497−499.
48. Neuhaus, D., and Williamson, M. P. (2000) *The Nuclear Overhauser Effect in Structural and Conformational Analysis*, Wiley-VCH, New York.

49. Wüthrich, K., Wagner, G., Richarz, R., and Perkins, S. J. (1978) Individual assignments of the methyl resonances in the 1H nuclear magnetic resonance spectrum of the basic pancreatic trypsin inhibitor, *Biochemistry 17*, 2253−2263.
50. Krishna, N. R., Aggresti, D. G., Glickerson, J. D., and Walter, R. (1978) Solution conformation of peptides by the intramolecular nuclear Overhauser effect experiment. Study of valinomycin-K+, *Biophys. J. 24*, 791−814.
51. Kumar, A., Ernst, R. R., and Wüthrich, K. (1980) A two-dimensional nuclear Overhauser enhancement (2D NOE) experiment for the elucidation of complete proton−proton cross-relaxation networks in biological macromolecules, *Biochem. Biophys. Res. Commun. 95*, 1−6.
52. Braun, W., Bosch, C., Brown, L. R., Go, N., and Wüthrich, K. (1981) Combined use of proton−proton Overhauser enhancements and a distance geometry algorithm for determination of polypeptide conformations. Application to micelle-bound glucagons, *Biochim. Biophys. Acta 667*, 377−396.
53. Wagner, G., Braun, W., Havel, T. F., Schaumann, T., Go, N., and Wüthrich, K. (1987) Protein structures in solution by nuclear magnetic resonance and distance geometry. The polypeptide fold of the basic pancreatic trypsin inhibitor determined using two different algorithms, DISGEO and DISMAN, *J. Mol. Biol. 196*, 611−639.
54. Bax, A. (1989) Two-dimensional NMR and protein structure, *Annu. Rev. Biochem. 58*, 223−256.
55. Feeney, J., Batchelor, G., Albrand, J. P., and Roberts, G. C. (1979) The effects of intermediate exchange processes on the estimation of equilibrium constants by NMR, *J. Magn. Reson. 33*, 519−529.
56. Feeney, J., Roberts, G. C., Thomson, J. W., King, R. W., Griffiths, D. V., and Burgen, A. S. (1980) Proton nuclear magnetic resonance studies of the effects of ligand binding on tryptophan residues of selectively deuterated dihydrofolate reductase from *Lactobacillus casei*, *Biochemistry 19*, 2316−2321.
57. Birdshall, B., Feeney, J., Pascual, C., Roberts, G. C., Kompis, I., Then, R. L., Muller, K., and Kroehn, A. (1984) A proton NMR study of the interactions and conformations of rationally designed brodimoprim analogs in complexes with *Lactobacillus casei* dihydrofolate reductase, *J. Med. Chem.* 27, 1672−1676.
58. Lian, L. Y., and Roberts, G. C. (1993) Effects of chemical exchange on NMR spectra, in *NMR of Macromolecules: A Practical Approach* (Roberts, G. C., Ed.) pp 153−182, Oxford University Press, Oxford, U.K.
59. Lian, L. Y., Barsukov, I. L., Sutcliffe, M. J., Sze, K. H., and Roberts, G. C. (1994) Protein−ligand interactions: exchange processes and determination of ligand conformation and protein−ligand contacts, *Methods Enzymol. 239*, 657−700.
60. Deng, H., Wu, J., So, S. P., and Ruan, K. H. (2003) Identification of the residues in the helix F/G loop important to catalytic function of membrane-bound prostacyclin synthase, *Biochemistry 42*, 5609−5617.
61. Piserchio, A., Zelesky, V., Yu, J., Taylor, L., Polgar, P., and Mierke, D. F. (2005) Bradykinin B2 receptor signaling: structural and functional characterization of the C-terminus, *Biopolymers 80*, 367−373.
62. Naider, F., Ding, F. X., VerBerkmoes, N. C., Arshava, B., and Becker, J. M. (2003) Synthesis and biophysical characterization of a multidomain peptide from a *Saccharomyces cerevisiae* G protein-coupled receptor, *J. Biol. Chem. 278*, 52537−52545.
63. Yeagle, P. L., Choi, G., Albert, A. D. (2001) Studies on the structure of the G-protein-coupled receptor rhodopsin including the putative G-protein binding site in unactivated and activated forms, *Biochemistry 40*, 11932−11937.
64. Gether, U. (2000) Uncovering molecular mechanisms involved in activation of G protein-coupled receptors, *Endocr. Rev. 21*, 90−113.
65. Hirata, T., Kakizuka, A., Ushikubi, F., Fuse, I., Okuma, M., and Narumiya, S. (1994) Arg60-to-leu mutation of the human thromboxane A2 receptor in a dominantly inherited bleeding disorder, *J. Clin. Invest. 94*, 1662−1667.
66. Flor, P. J., Gomeza, J., Tones, M. A., Kuhn, R., Pin, J. P., and Knopfel, T. (1996) The C-terminal domain of the mGluR1 metabotropic glutamate receptor affects sensitivity to agonists, *J. Neurochem. 67*, 58−63.
67. Heller, R. S., Kieffer, T. J., and Habener, J. F. (1996) Point mutations in the first and third intracellular loops of the glucagon-like peptide-1 receptor alter intracellular signaling, *Biochem. Biophys. Res. Commun. 223*, 624−632.
68. Tseng, C. C., and Lin, L. (1997) A point mutation in the glucose-dependent insulinotropic peptide receptor confers constitutive activity, *Biochem. Biophys. Res. Commun. 232*, 96−100.
69. Wu, V., Yang, M., McRoberts, J. A., Ren, J., Seensalu, R., Zeng, N., Dagrag, M., Birnbaumer, M., and Walsh, J. H. (1997) First intracellular loop of the human cholecystokinin-A receptor is essential for cyclic AMP signaling in transfected HEK-293 cells, *J. Biol. Chem. 272*, 9037−9042.
70. Arora, K. K., Krsmanovic, L. Z., Mores, N., O'Farrell, H., and Catt, K. J. (1998) Mediation of cyclic AMP signaling by the first intracellular loop of the gonadotropin-releasing hormone receptor, *J. Biol. Chem. 273*, 25581−25586.
71. Nakamura, K., Hipkin, R. W., and Ascoli, M. (1998) Mediation of cyclic AMP signaling by the first intracellular loop of the gonadotropin-releasing hormone receptor, *Mol. Endocrinol. 12*, 580−591.
72. Naro, F., Perez, M., Migliaccio, S., Galson, D. L., Orcel, P., Teti, A., and Goldring, S. R. (1998) Phospholipase D- and protein kinase C isoenzyme-dependent signal transduction pathways activated by the calcitonin receptor, *Endocrinology 139*, 3241−3248.
73. Calandra, B., Portier, M., Kerneis, A., Delpech, M., Carillon, C., Fur, G. L., Ferrara, P., and Shire, D. (1999) Dual intracellular signaling pathways mediated by the human cannabinoid CB1 receptor, *Eur. J. Pharmacol. 374*, 445−455.
74. Cypess, A. M., Unson, C. G., Wu, C. R., and Sakmar, T. P. (1999) Two cytoplasmic loops of the glucagon receptor are required to elevate cAMP or intracellular calcium, *J. Biol. Chem. 274*, 19455−19464.
75. Appleyard, S. M., McLaughlin, J. P., and Chavkin, C. (2000) Tyrosine phosphorylation of the kappa-opioid receptor regulates agonist efficacy, *J. Biol. Chem. 275*, 38281−38285.
76. Jap, T. S., Wu, Y. C., Jenq, S. F., and Won, G. S. (2001) A novel mutation in the calcium-sensing receptor gene in a Chinese subject with persistent hypercalcemia and hypocalciuria, *J. Clin. Endocrinol. Metab. 86*, 13−15.
77. Jackson, A., Iwasiow, R. M., Chaar, Z. Y., Nantel, M. F., and Tiberi, M. (2002) Homologous regulation of the heptahelical D1A receptor responsiveness: specific cytoplasmic tail regions mediate dopamine-induced phosphorylation, desensitization and endocytosis, *J. Neurochem. 82*, 683−697.
78. Liu, B., and Wu, D. (2003) The first inner loop of endothelin receptor type B is necessary for specific coupling to Galpha 13, *J. Biol. Chem. 278*, 2384−2387.
79. McCoy, M. A., and Wyss, D. F. (2000) Alignment of weakly interacting molecules to protein surfaces using simulations of chemical shift perturbations, *J. Biomol. NMR 18*, 189−198.
80. Onrust, R., Herzmark, P., Chi, P., Garcia, P. D., Lichtarge, O., Kingsley, C., and Bourne, H. R. (1997) Receptor and betagamma binding sites in the alpha subunit of the retinal G protein transducin, *Science* 275, 381−384.
81. Katsuyama, M., Sugimoto, Y., Namba, T., Irie, A., Negishi, M., Narumiya, S., and Ichikawa, A. (1994) Receptor and betagamma binding sites in the alpha subunit of the retinal G protein transducin, *FEBS Lett. 344*, 74−78.
82. Miggin, S. M., and Kinsella, B. T. (2002) Investigation of the mechanisms of G protein: effector coupling by the human and mouse prostacyclin receptors. Identification of critical species-dependent differences, *J. Biol. Chem. 277*, 27053−27064.

BI050483P